Effects of Extensional Rates on Characteristic Scales of Two-dimensional Turbulence in Polymer Solutions

R Hidema[1]*****
Organization of Advanced Science and Technology, Kobe University,
1-1, Rokkodai, Nada, Kobe, Hyogo, Japan. 657-8501

E-mail: hidema@port.kobe-u.ac.jp

Abstract. In order to study the effects of extensional viscosities on turbulent drag reduction, experimental studies using two-dimensional turbulence have been made. Anisotropic structures and variations of energy transfer induced by polymers are considered. Polyethyleneoxide and hydroxypropyl cellulose having different flexibility, which is due to different characteristics of extensional viscosity, are added to 2D turbulence. Variations of the turbulence were visualized by interference patterns of 2D flow, and were analysed by an image processing. The effects of polymers on turbulence in the streamwise and normal directions were also analysed by 2D Fourier transform. In addition, characteristic scales in 2D turbulence were analysed by wavelet transform.

1. Introduction

Addition of little amounts of flexible polymers to turbulent flows reduces the friction coefficients to solid walls in the flow. Such drag reduction phenomena have been studied for many decades. One of the key of this effect is the increase of extensional viscosity that is due to the extension of polymers in the flow [1-3]. Rheological effects such as the extensional viscosity have been studied in numerical studies [3,4]. Since the extensional viscosity stems from the resistance in the extensional direction, the effects cause anisotropic structures in turbulence. Therefore, turbulence affected polymers is not uniformly decayed in space, that is, the effects in the streamwise directions can be different from those in normal direction. Such anisotropic effects have been investigated by many numerical analyses, but not enough experimental studies have been made [5]. In addition, it is difficult to separate the effects of extensional stress from those of shear stress on polymers in conventional three dimensional pipe experiments.

Therefore, we have been used self-standing flowing soap films as a test bed for two-dimensional (2D) flow [1,2,6]. The soap films consist of water layer and surfactant molecules covering the surface, which flows between two parallel nylon wires. Since the surfactant molecules are really small compared to the thickness of water layer, the flowing soap films are considered to be a water layer sandwiched by free surface. Thus, the shear stress is very small in this system. When a grid is inserted to the flow, 2D grid turbulence is generated in the flow. Extensional stress is generated at the

*Corresponding author: R Hidema
Phone: +81-78-803-6657, Fax: +81-78-803-6657
E-mail address: hidema@port.kobe-u.ac.jp

grids, and therefore, when polymers exist in the flow, the turbulence affected mainly the extensional viscosity of polymers due to the extensional stress can be observed.

In this study, the effects of the extensional rate on anisotropic structures of 2D turbulence, which is induced by the extensional flow of polymer solution, have been examined. Polyethyleneoxide (PEO) and hydroxypropyl cellulose (HPC) are added to the 2D turbulence respectively. PEO is a flexible polymer and HPC is a rigid rod-like polymer, which show different characteristics of the extensional viscosity. Turbulence affected polymers are analysed by an image processing to investigate how and why anisotropic structures appear and characteristic scales of turbulence are changed by flexibility and extensional viscosity of polymers.

2. Experimental procedures

2.1. Materials

Soap solutions contain sodium dodecylbenzenesulfonate (SDBS) as a surfactant at a concentration of 2 wt%. As a flexible polymer, polyethyleneoxide (PEO, molecular weight: 3.5×10^6) is used at concentrations of 0.25, 0.5, 0.75, 1.0, 1.5, and 2.0×10^{-3} wt%. As a rigid polymer, hydroxypropyl cellulose (HPC, molecular weight: $>1.0\times10^6$) is used at concentrations of 0.01, 0.03, and 0.05 wt%.

2.2. Visualization of two-dimensional turbulence by flowing soap films

The apparatus used for experiments is shown in figure 1. Whole image of the apparatus is shown in figure 1(a). The outline of our apparatus follows that proposed by Rutgers *et al.* [7]. Two nylon wires tightened by a weight were used to make a soap film channel. Sample solutions containing surfactant flowed between the two nylon wires from a top reservoir to a bottom reservoir by gravity. The flow reached uniform velocities at about 30 cm behind from the injection nozzle. In this study, the mean velocity was 130 cm/s. The mean thickness of the water layer was approximately 3.85μm, with a mean velocity of 130 cm/s for a flow flux of 0.5 ml/s. At a grid of equally spaced cylinders, vortices were generated and were convected without much deformation to the observation area where about 20 cm under the grid. Illumination light was reflected at the front and the back of the flowing soap films, which made the interference images (figure 1(c)). The interference images were related to the thickness of the water layer. Therefore, the dynamics of the flow was visualized through the interference patterns. A digital video camera (Panasonic TM700) was used to record the flow in the data acquisition area (figure 1(b)).

2.3. Extensional Rate Added at a Grid

When the flow passes the grid, local velocities were increased at the grid since the cross-section area of the water layer was decreased. The sudden increase of the local velocity between the cylinders induces the extensional rate that described as follows.

$$S(t) = S_0 \exp(-\dot{\varepsilon}t) \tag{1}$$

where S_0 m^2 is the cross-section area before deformation, $S(t)$ m^2 is the cross-section area after deformation, t s is the time required for deformation, and $\dot{\varepsilon}$ s^{-1} is the apparent extensional rate. The extensional rate was controlled by the distance between cylinders and its diameter. In the present study, the diameter of the cylinder was 0.3 cm. The distances between two cylinders were 0.9 cm or 0.6 cm as shown in figure 1(d). The numbers of the cylinders were changed seven to eight for each distance. Concretely speaking, when the number of the cylinders were seven and the distances were 0.9 cm, S_0 m^2 was 7.20 cm x 3.85 μm and $S(t)$ m^2 was 5.40 cm x 3.85 μm. Thus, $\dot{\varepsilon}$ was approximately 250 s^{-1}. When the distances between cylinders were 0.6 cm, $\dot{\varepsilon}$ was 350 s^{-1}. These extensional rates affect polymers. Polymers are considered to be stretched and to be oriented in the flow, which induce extensional viscosity. This affects the generation of vortices in 2D turbulence.

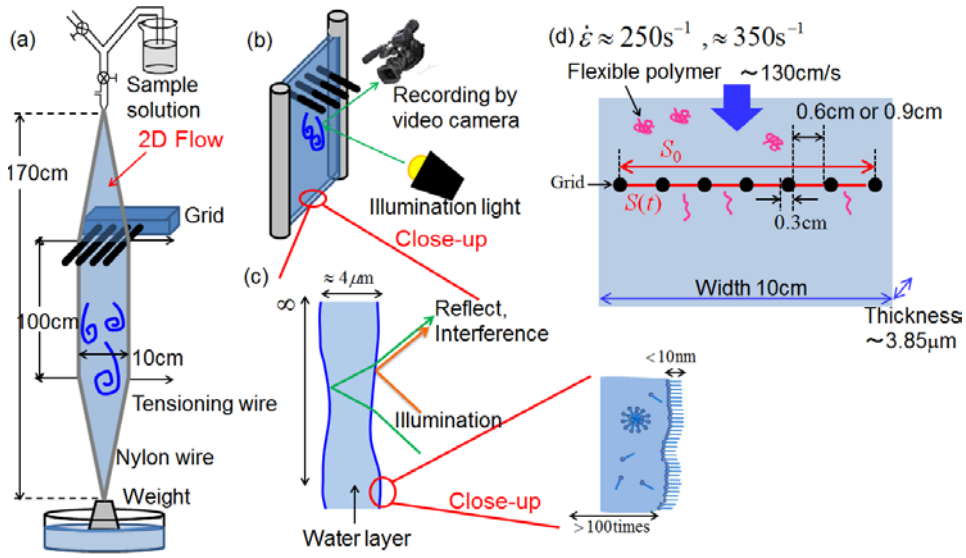

Figure 1. Apparatus of flowing soap films.

3. Image processing by Film Interference Flow Imaging

The interference patterns of the flowing soap films as 2D turbulence were analysed by image processing methods. Such a method using interference patterns to obtain quantified information of 2D flow is unique. Therefore, we called this method "Film Interference Flow Imaging (FIFI)" in our previous study [8].

3.1. Two-dimensional fast Fourier transform (2D-FFT)

2D-FFT software was used to calculate power spectra of the interference images. Since the Red-Green-Blue (RGB) pixel intensity of images are related to the thickness of the water layer, the power spectra of the images show the dynamics of 2D flow. In the present study, the power spectrum $<I^2(k_x, k_y)>$ was calculated based on the pixel intensity of G with a Hamming window, where k_x m^{-1} and k_y m^{-1} are the spatial frequency in the normal and streamwise directions in an interference image. The pixel intensity of G was chosen to avoid variation of an order of interference in the data acquisition area. The area is 256 pixels × 256 pixels, which correspond to about 2.56×2.56 cm^2. Therefore, k_x and k_y range from about 1/2.56 to 1/0.02 cm^{-1}, i.e., 0.391 cm^{-1} to 5.00 cm^{-1} as the frequency.

An example of the power spectrum $< I^2(k_x, k_y)>$ of the interference pattern at the extensional rate of 250 s^{-1} is shown in figure 2(a) and (b). Figure 2(a) shows a 2D representation of $<I^2(k_x, k_y)>$ in the case of polymer free solution, where the darkness of the image indicates the intensity. Two arrows in the image indicate the directions corresponding to the streamwise and normal directions in the interference patterns. Figure 2(b) is the power spectrum represents $< I^2(k_x, 0) >$, which shows the scaling behaviors. The scaling index was used to discuss the energy transfer in 2D turbulence.

3.2. Wavelet transform

Sequence pixel intensities in the streamwise direction were analysed by a wavelet transform to investigate the spatial fluctuation of the water layer [9]. Contrary to the Fourier transform, the wavelet transform can resolve strongly irregular signals, such as turbulent signals from different scales, while keeping the signals localized both in space and frequency. Wavelet analysis provides a 2D unfolding of one-dimensional signals, resolving both the position and the scale as independent variables [10]. The analysed sequence pixels were approximately 6,000 pixels corresponding to 65 cm. The sequence intensities of G in the image were obtained by connecting consecutive images as shown in figure 2(c).

The wavelet transform coefficient, $W(a, b)$, is defined for the intensity of G in the streamwise direction, $G(x)$.

$$W(a,b)=\frac{1}{\sqrt{a}}\int\varphi\left(\frac{x-b}{a}\right)G(x)dx \quad (1)$$

where x m is the length scale in the streamwise direction, and a m and b m are the wavelet scale and the sequence scale parameters, respectively. The function $\varphi(x)$ is defined as a mother wavelet, which is localized around $x = 0$. In the present study, the mother wavelet, $\varphi(x)$, is a Mexican hat. The fluctuation in the sequence data was resolved by the wavelet transform to the position and magnification which correspond to x and a^{-1}. As a result, wavelet coefficients of sequence intensities were plotted on the wavelet scale, a m, and a sequence scale, b m. Here, b m is related to the analysed distance in the streamwise direction 65 cm, that is, sequence 6,000 pixels. Figure 2(d) shows an example of the result. Bright part of the image corresponds to positive correlations, and dark part of the image corresponds to negative correlations. In addition, the root mean square values of the wavelet coefficients, W_{rms}, normalized by a difference between the maximum and minimum values of the wavelet coefficients, $W_{max\text{-}min}$, are plotted on the wavelet scale, a m (figure 2(e)). As an example, a periodic structure seen at a wavelet scale a m shown by the arrow in figure 2(d) corresponds to the peak intensity shown in figure 2(e).

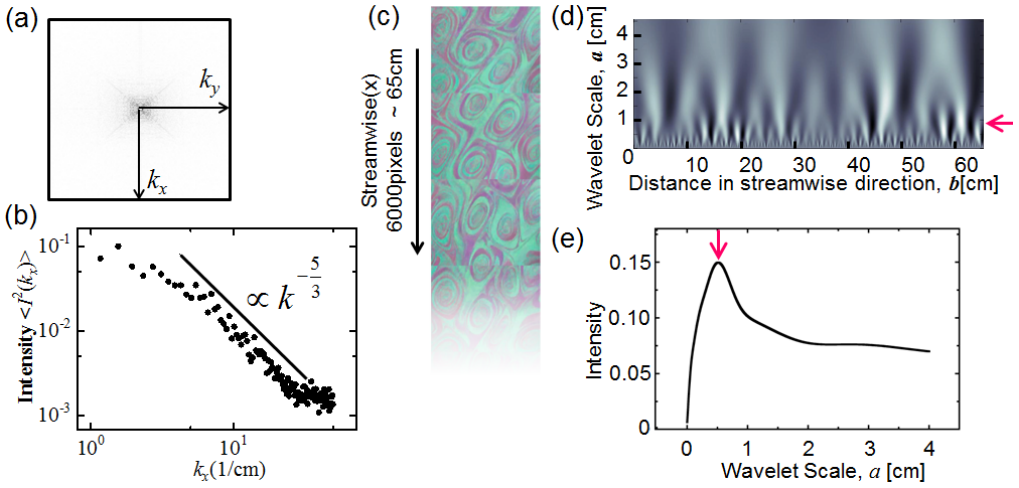

Figure 2. (a) 2D representation of the power spectrum. The k_x and k_y directions in the image represent the spatial frequencies in the streamwise and normal directions. (b) A power spectrum. (c) Schematic of sequence pixel intensity. (d) A wavelet coefficient. (e) W_{rms} normalized by $W_{max\text{-}min}$ plotted on the wavelet scale, a m.

4. Results and discussion

Figure 3 shows interference images of the 2D turbulence in flowing soap films when the extensional rate, $\dot{\varepsilon}$ s^{-1}, is 250 s^{-1}. In the case of polymer free solution, the size of the vortices in turbulence is about 1 cm in diameter as shown in figure 3(a). In 2D flow, energies transfer from smaller scale to larger scale. This phenomenon is called inverse energy cascade, since the direction of the energy transfer is opposite to 3D case. In figure 3(a), energies transfer from smaller scale to larger scale, therefore, the vortices can grow. On the other hand, the vortices become long and thin with the addition of PEO as shown in figure 3 (b) to (d). When the concentration of PEO is 2.0 x 10^{-3} wt%, vortices are hardly seen. This is considered to be a manifestation of the prohibition of the inverse energy cascade that is caused by PEO. The energy stays in smaller scales as fluctuations. Therefore, the vortices could not grow. Figures 3(e) to (g) show for the case of HPC. The vortices are deformed

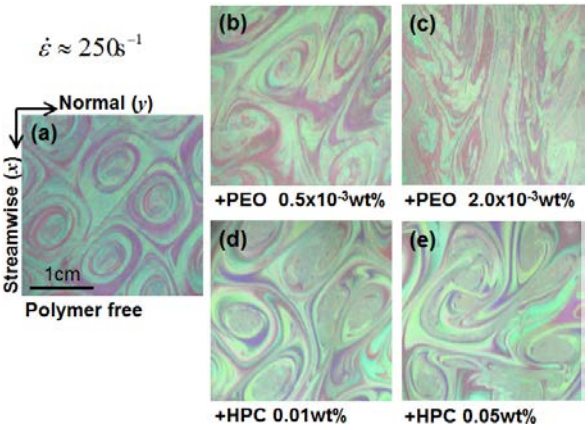

Figure 3. Interference images of the turbulence in flowing soap films when $\dot{\varepsilon}$ [s^{-1}] was 250 s^{-1}.

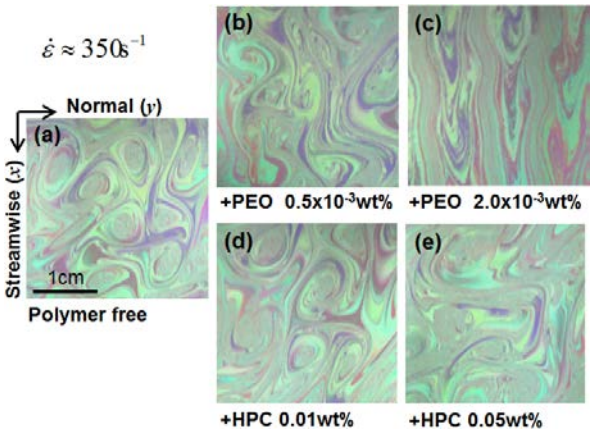

Figure 4. I Interference images of the turbulence in flowing soap films when $\dot{\varepsilon}$ [s^{-1}] was 350 s^{-1}.

by adding HPC, however, the results seems different. In the case of PEO, the vortices are stretched in the streamwise direction, which does not necessarily apply to HPC case. Figure 4 shows interference image when $\dot{\varepsilon}$ s^{-1} is 350 s^{-1}. The effect of PEO seems to be increased even at the same concentration, which is true of HPC case.

Here, the interference patterns visualize the thickness of water layer related to the vortices in 2D flow. The thickness is considered as a passive scalar in 2D flow. The power spectrum of the passive scalar is affected by inverse energy cascade in 2D flow. Thus, scaling exponent obtained from the power spectrum of the interference patterns indicate the mechanism of energy transfer in 2D turbulence. Figure 5 shows the scaling exponents of PEO added solutions in the streamwise and normal directions. The scaling exponents of polymer free solution were almost -5/3 in the both directions and the both extensional rates, which is predicted as passive scalar scaling when inverse energy cascade exists in the flow. Figure 5(a) shows that the scaling components approach to -1 when the concentration of

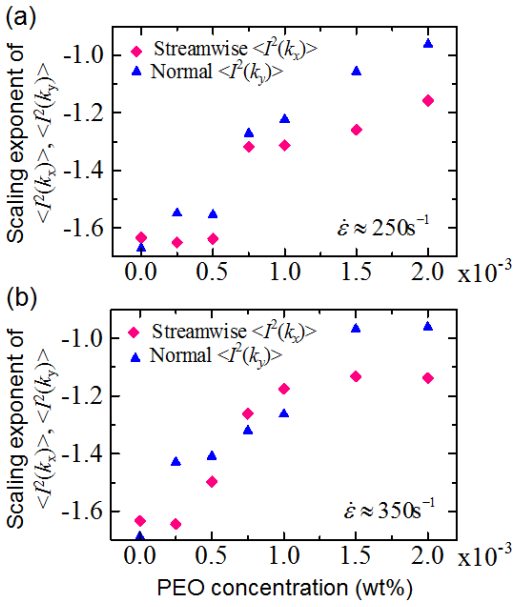

Figure 5. Scaling exponent of PEO added solution at each extensional rate.

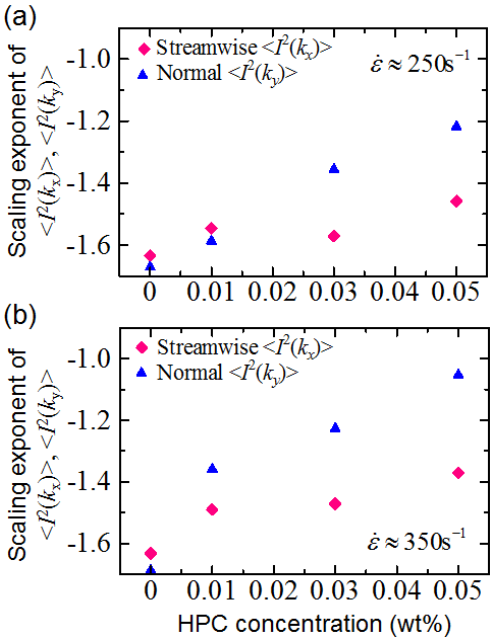

Figure 6. Scaling exponent of HPC added solution at each extensional rate.

PEO is increased. In addition, the variation is large at 0.75 x 10^{-3} wt% in both directions. This critical concentration is shifted to lower concentration when the extensional rate is higher (figure 5(b)). The scaling exponent of passive scalar of -1 indicates that the inverse energy cascade ceased because of the existence of polymers. Figure 6 shows the case of HPC added solutions. When $\dot{\varepsilon}$ s^{-1} is 250 s^{-1}, the scaling exponent gradually approaches to -1 in the normal direction, while the variation is very small in the streamwise direction (figure 6(a)). When the extensional rate is higher, the variations of the scaling exponents are larger (figure 6(b)). The results of figure 5 and 6 indicate that the inverse energy transfer is prohibited by adding PEO and HPC. However the effect is considered to be different. At the grid inserted in the flow, flexible PEO is expected to be suddenly stretched and oriented parallel to the streamwise direction. The orientation could prohibit energy transfer in the normal direction. Thus, the effect was seen in the normal direction well. In the streamwise direction, the extensional viscosity of PEO may be related to the prohibition of the energy transfer, since PEO exhibit extensional viscosity in the extension direction. In general, extensional viscosity is higher when a polymer is flexible and when the extensional rate is higher. Therefore, the effects of PEO in

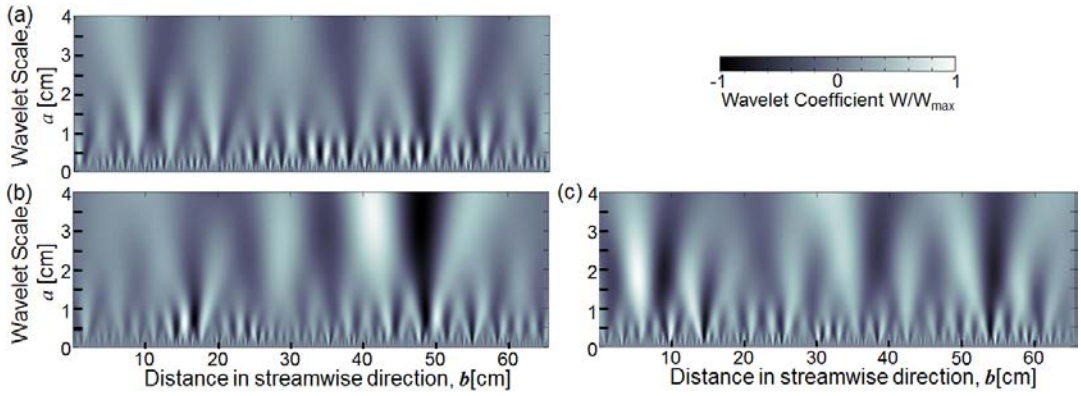

Figure 7. Wavelet coefficient contours for interference images of (a) SDBS 2 wt% solution, (b) + PEO 2.0 x 10^{-3} wt%, (c) + HPC 0.05 wt% when the extensional rate is 250 s^{-1}.

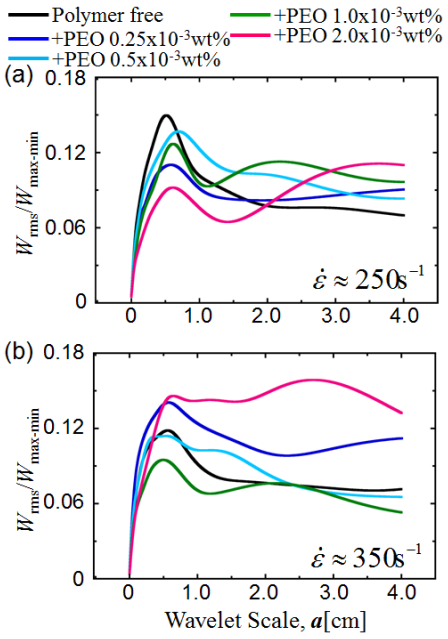

Figure 8. The root mean square value of the wavelet coefficient of the PEO added solution.

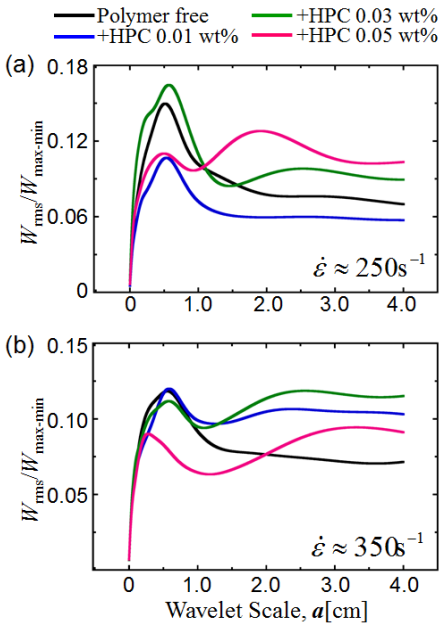

Figure 9. The root mean square value of the wavelet coefficient of the HPC added solution.

the streamwise direction are larger than that of rigid HPC. HPC is also expected to be oriented parallel to the streamwise direction. Therefore, HPC can prohibit energy transfer in the normal direction. However, the extensional viscosity of HPC is smaller, thus the effect is smaller in the streamwise direction.

Since the streamwise direction was considered to be affected by extensional viscosities, the fluctuation in the streamwise direction was analysed by wavelet transform. Figure 7 shows the wavelet coefficient contour for each solution. In the case of polymer free solution, relatively strong periodic structure is seen at smaller than 1 cm of the wavelet scale (figure 7(a)). When PEO induces laminaliztion of the 2D turbulence, the periodic structure at smaller than 1 cm of the wavelet scale

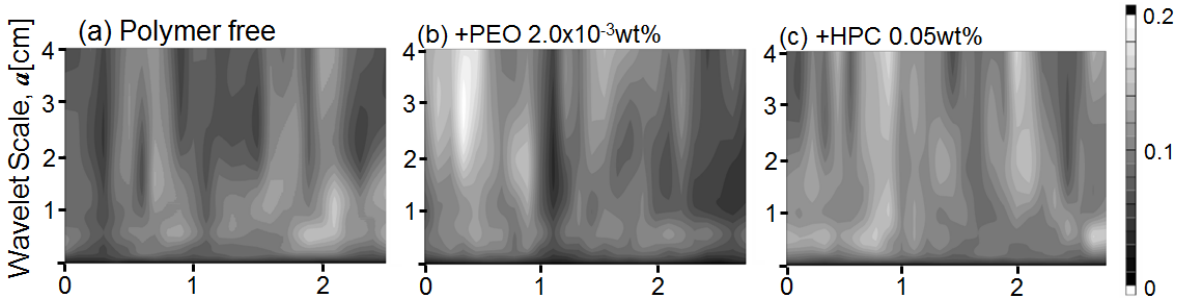

Figure 10. Mapping of $W_{rms}/W_{max\text{-}min}$ of each solution.

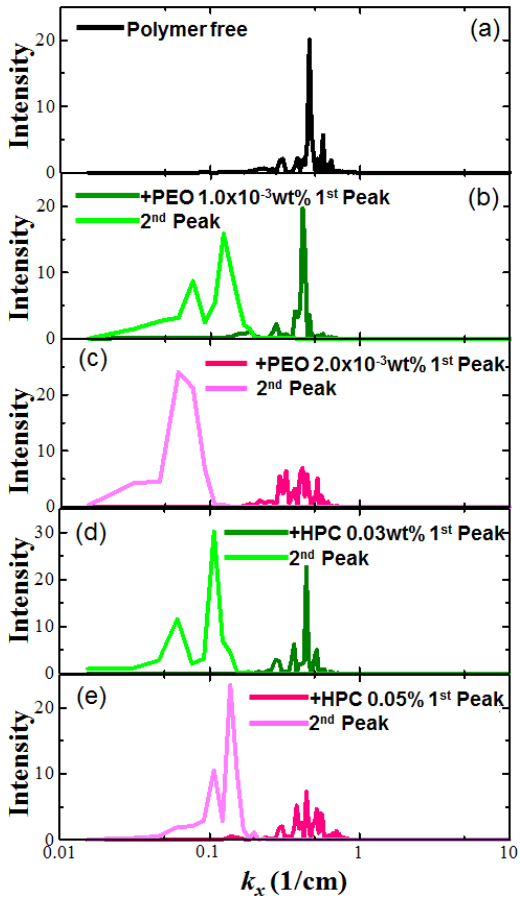

Figure 11. Power spectra of wavelet coefficients of each solution. $\dot{\varepsilon}$ s^{-1} is 250 s^{-1}.

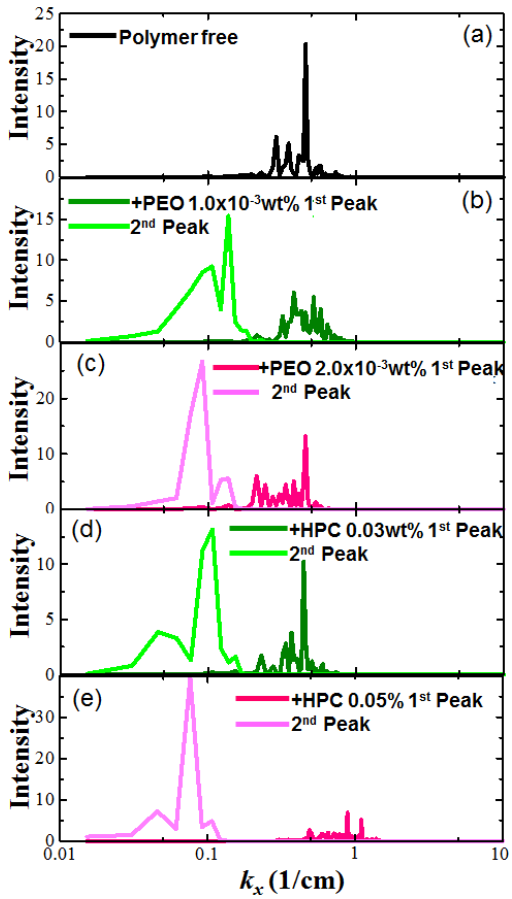

Figure 12. Power spectra of wavelet coefficients of each solution. $\dot{\varepsilon}$ s^{-1} is 350 s^{-1}.

becomes weak, while a strong variation is seen at about 3 cm of the scale (figure 7(b)). In the case of HPC added solution, 7(c), the tendency seems to be the same as figure 7(b). In order to determine how the periodic structures are changed by polymer concentration, the normalized root mean square values of the wavelet coefficients, $W_{rms}/W_{max\text{-}min}$ was calculated (figure 8. 9). The peak of the polymer free case shown in figure 8(a) appears at the wavelet scale corresponding to the scale where the original fluctuation due to the original vortices was observed. When the concentration of PEO is increased, the original peak becomes relatively smaller while the other wider peak appears at the larger scale as shown in figure 8(a). The peak appears at the larger scale is related to the periodic structure in the larger scale. The wider peak is shifted to a larger scale by increasing the concentration of PEO when $\dot{\varepsilon}$ s^{-1} is 250 s^{-1}. The results fit to a previous study suggesting that the addition of PEO affects larger scale than an injection scale in 2D turbulence [6]. The phenomenon is also observed in 350 s^{-1} (figure 8(b)). These tendencies are similar in HPC added solution (figure 9). However, the wider peak appears randomly in the case of HPC added solution. Figures 7 to 9 are obtained by a wavelet transform of a single line in the streamwise direction of an image. Therefore, 25 streamwise lines, 10 pixel spaced in 256 pixels in the normal direction, were analysed by the wavelet transform to observe how $W_{rms}/W_{max\text{-}min}$ was changed at each line. The results are shown in figure 10 as a mapping of $W_{rms}/W_{max\text{-}min}$. The tendency of each line is similar in the same solution. Therefore, to pick up a characteristic line is reasonable as a first trial. Thus the variations of the periodic structure at the peak of the original wavelet scale and the peak of the larger wavelet scale are analysed by Fourier transform. The results shown in figure 11 and 12 indicate clearly the dissipation of the original peak and appearance of the second wider peak. The second peak is enhanced by increasing the polymer concentration, which determines the larger scale fluctuation due to flow laminalization by polymer.

5. Conclusions

In order to investigate effects of extensional viscosity of polymers on turbulent drag reduction, polymer-added 2D turbulence was observed. Flexible PEO and rigid HPC showing different characteristics of extensional viscosity were added to the 2D turbulence. From the results of 2D-FFT of the interference patterns, it was suggested that the effects of polymers in the streamwise and normal directions were different. Orientation of polymer prohibits energy transfer in the normal direction, while extensional viscosity prohibits energy transfer in the streamwise direction. Fluctuations in the streamwise direction were precisely analysed by wavelet transform. From the results, it was revealed that original vortices in 2D turbulence disappear and fluctuations even in a larger scale appear when flow laminarization occurs due to polymers.

6. References

[1] Hidema R, Suzuki H, Hisamatsu S, Komoda Y and Furukawa H 2013 *Rheol. Acta.* **52** 949
[2] Hidema R, Suzuki H, Hisamatsu S and Komoda Y 2014 *AIChE J.* **60** 1854
[3] Tamano S, Itoh M, Hoshizaki K and Yokota K 2007 *Phys. Fluids.* **19** 075106-1
[4] Housiadas K D and Beris A N 2004 *J. Non-Newtonian Fluid Mech.* **122** 243
[5] Housiadas K D and Beris A N 2004 *Phys. Fluids.* 16 1581
[6] Kellay H and Goldburg W I 2002 *Rep. Prog. Phys.* **65** 845
[7] Rutgers M A, Wu X L and Daniel W B 2001 *Rev. Sci. Instrum.* **72** 3025
[8] Hidema R, Ushiki H and Furukawa H 2011 *J. Solid Mech. Mater. Eng.* **5** 838
[9] Suzuki H, Nguyen H-P, Nakayama T and Usui H 2005 *Rheol. Acta.* **44** 457
[10] Do-Khac M, Basdevant C, Perrier V and Dang-Tran K 1994 *Physica D.* **76** 252